*Int. J. Electrochem. Sci.*, 16 **(2021)** Article ID: 210929, doi: 10.20964/2021.09.40

International Journal of
ELECTROCHEMICAL
SCIENCE
www.electrochemsci.org

# Impact of Conyza bonariensis extract on the corrosion protection of carbon steel in 2 M HCl solution

*K.J. Al-Sallami*[1,2], *K. Shalabi*[1], *A.S. Fouda*[1,*]

[1] Chemistry Department, Faculty of Science, Mansoura University, Mansoura, Egypt
[2] Chemistry Department, Faculty of Science, Mustansiriyah University, Baghdad, Iraq
[*]E-mail: asfouda@hotmail.com

*Received:* 25 xMay 2021 / *Accepted:* 1 July 2021 / *Published:* 10 August 2021

Herein, we study the use of *Conyza bonariensis* extract as eco-friendly corrosion inhibitor for carbon steel (CS) in 2 M HCl. This study was evaluated by weight loss (WL), electrochemical frequency modulation (EFM), potentiodynamic polarization (PP), and electrochemical impedance spectroscopy (EIS). The morphology of inhibited carbon steel was analyzed by scanning electron microscope (SEM), energy-dispersive X-ray spectroscopy (EDX) and Atomic Force Microscopy (AFM). Results obtained indicated that the inhibition efficiency was improved by increasing the concentration of *C. bonariensis* and decreased by raising the temperature. PP curves showed the ability of C. *bonariensis* plant to serve as a mixed-type inhibitor. Moreover, the EIS results confirmed that the adsorption of *C. bonariensis* on CS surface by lowering the values of double layer capacitance ($C_{dl}$) and increasing the values of charge transfer resistance ($R_{ct}$) with increasing of the concentration. All tests gave almost similar results.

**Keywords:** Corrosion inhibition; Carbon steel; HCl; *Conyza bonariensis*; EIS; SEM; AFM

## 1. INTRODUCTION

The metals corrosion is one of the extremely important issues that need to study to understand how to protect it from corrosion because of the resulting problems, as the economic losses because of material degradation. Corrosion can be defined as a deterioration and degradation of metals and by chemical and electrochemical reactions which affects all areas of the environment [1-2]. Carbon steel (CS) can be considered as one of the most significant materials used for petroleum purposes, tanks, pipelines, equipment of ships, and other industries because of its outstanding properties such as low cost, easy to manufacture, and keep its properties at high temperature. Unfortunately, CS is recumbent to corrosion when contact with acidic solutions that is why many studies are focusing on this issue [3-6].

Inhibitors are the most practical materials methods which can be used for protection against corrosion, practically in acidic media. Green inhibitor can be conceded as the best protection methods due to its many advantages for examples: availability with low cost, renewable resources, and environmental safety. Many studies were exercised on corrosion protection by nature products [7-10]. Many plant extracts have been successfully improved their activity on the degradation of CS within acidic environments [11-20]. *Conyza bonariensis* (*C. bonariensis*) is one of the plant species belongs to genus *Conyza*, family Asteraceae which has many pharmacological applications including treatment of smallpox, sore throat, skin-related diseases, toothache, headache, rheumatism, and cystitis [21-23]. The *C. bonariensis* extract was used as inhibitor because its price is low, and it does not affect the environment. In this study, we investigate the inhibition activity of *C. bonariensis* extract on the CS corrosion with 2 M HCl. The techniques used for the current study were WL and electrochemical tests. The adsorption of *C. bonariensis* extract on the CS surface has been proved and characterized by Atomic Force Microscopy (AFM) and Scanning Electron Microscope (SEM).

## 2. EXPERIMENTAL

### *2.1. Materials and Methods*

#### *2.1.1 Composition of CS Samples*

The CS samples which used in the experiments are having the following composition: 0.15 %Cr, 0.52 %Si, 16.41 %C, 0.39 % Mn, 3.75 %Tb and Fe rest. The dimension of the specimens is 2 x 2 x 0.2 cm. Before starting measurements, the samples must be treated by various grades of emery papers then washed them by double distilled water and dried.

#### *2.1.2. Preparation of Corrosive Media*

The destructive solution used in the study was 2 M HCl which prepared by diluted analytical reagent grade HCl (37%) by double distilled water.

#### *2.1.3. Preparation of Plant Extracts*

After collection of *C. bonariensis* leaves, we dried them at room temperature and ground into a fine powder by using an electrical mill. Take about two hundred grams (200 g) of this powder and soaked into 800 ml of methanol, at a ratio of 1:4 (powder/solvent). Under vacuum the extract was isolated then dried by rotary evaporator. The investigated extract was liquefied in ethanol (1 g/L) and stored into the refrigerator. Previous investigations of *C. bonariensis* have revealed glycosides, polyphenolic compounds, flavonoids and sesquiterpenic lactones [24-25].

*2.2. Weight Loss (WL) Method*

At first the CS specimens must be physically treated before starting the study by emery papers of various grades which abraded to finish a mirror then washed by double distilled water and dried by filter papers. Samples were weighted by electrical balance. The concentrations used of *C. bonariensis* extract were varied from 10 to 100 ppm. The coupons were dipped into a solution of 100 ml of 2 M of HCl in the absence and presence of various *C. bonariensis* extract concentrations for 180 min. The immersion time is 30 min where, the samples were weighted again. The rates of corrosion (CR), the surface coverage (θ) and the inhibition efficacy (%$IE_{WL}$) acquired from the WL method were counted from the following equations. [26, 27]:

$$CR = \frac{M}{At} \quad (1)$$

$$\theta = \frac{CR - CR_{(i)}}{CR} \quad (2)$$

$$\%IE_{WL} = \theta \times 100 \quad (3)$$

where "M is the reduction in mass (mg), $CR_{(i)}$ and CR are the rates of corrosion with and without extract, respectively, t is the immersion time (min), and A is the area of the surface ($cm^2$)".

*2.3. Electrochemical Techniques*

Three different electrodes are placed together in a glass cell for electrochemical measurements. A reference electrode which is $Ag/AgCl_{(s)}$ electrode, platinum wire is auxiliary electrode, and the working electrode is made from CS with exterior area 10 $mm^2$. The surface of working electrode must be physically treated in the same approach as WL method [28]. Before starting a measurement, CS electrode placed in the studied solution for 20 min to attain a steady state (OCP). For PP tests, the applied potential was from -0.5 to + 0.5 V at (OCP) with scan rate 0.5 $mVs^{-1}$. The current of corrosion $i_{corr}$ was evaluated from the extrapolating of anodic and cathodic ($\beta_a$ & $\beta_c$) Tafel slopes to obtain $i_{corr}$, to measure IE% of the inhibitor and (θ) we used the following relation [29]:

$$\%IE_{PDP} = [\,1 - \frac{i_{corr(inh)}}{i_{corr(free)}}] \times 100 \quad (4)$$

Where "$i_{corr\ (free)}$ and $i_{corr\ (inh)}$ are the current densities without and with inhibitors, respectively". The impedance tests (EIS) were done with frequency diversity of 100 kHz to 0.2 Hz peak-to-peak amplitude of 10 mV at (OCP). The %IE is calculated from this formula [30]:

$$\%IE_{EIS} = [\,1 - \frac{R_{ct(free)}}{R_{ct(inhi)}}] \times 100 \quad (5)$$

wherever "$R_{ct\ (free)}$ and $R_{ct\ (inh)}$ are the resistances of charge transfer for absence and presence of inhibitors" respectively.

*2.4. Examination of the Surface by AFM, SEM*

In the absence and presence of 100 ppm *C. bonariensis* extract, the CS sample under study was immersed in a 2 M HCL solution. After 24 hours, the sample was taken out and allowed to air dry at room temperature, and then the morphological surface of the CS samples was calculated by atomic force

microscopy (AFM). Use Scanning Electron Microscope (SEM) and Energy Dispersive X-ray Spectroscopy (EDX) to calculate the thin film formed on the CS surface with different wave numbers ranging from 10 to 50 mm.

## 3. RESULTS AND DISCUSSION

### *3.1. Weight Loss (WL) Measurements*

#### *3.1.1. Effect of Concentration and Temperature*

The corrosion rate (CR) of studied CS was determined before and after added different concentrations of *C. bonariensis* extract by calculating the WL per area per unit time. The mass of CS samples measured prior to and after immersion time for 180 min in the uninhibited and inhibited corrosive solution by electrical balance. WL curves against time at 30 °C for CS in 2 M HCl before and after adding various concentrations of *C. bonariensis* extract was shown in Fig.1. WL measurements were done at various temperatures of 30, 35, 40 and 45 °C. The impact of temperature on the CR of CS in the absence and presence of various concentrations of investigated extract was shown in Table 1. From the data in this table, we noticed that the CR was diminished with raising the concentration of investigated inhibitor, so, the %IE increases. This occurs by virtue of the adsorption of *C. bonariensis* extract on the surface of CS and by raising the concentration of the *C. bonariensis* plant extract leads to raising the surface coverage (θ) of extract on the surface of CS and forming a layer of studied extract on CS which protects it from destroyed [32,33]. By increasing the temperature, the CR decreases and the %IE of the *C. bonariensis* plant extract increases as shown in Table 1 indicating that the adsorption of plant extract is physisorption.

**Table 1.** Effect of various concentrations of *C. bonariensis* on CR and IE % of CS in 2 M HCl at various temperatures.

| **Inh.** | concentration, ppm | **30.0°C** | | **35.0°C** | | **40.0°C** | | **45.0°C** | |
|---|---|---|---|---|---|---|---|---|---|
| | | CR×10$^{-2}$ mgcm$^{-2}$min$^{-1}$ | %IE | CR×10$^{-2}$ mgcm$^{-2}$min$^{-1}$ | %IE | CR×10$^{-2}$ mgcm$^{-2}$min$^{-1}$ | %IE | CR×10$^{-2}$ mgcm$^{-2}$min$^{-1}$ | %IE |
| *C. bonariensis* | 2 M HCl | 0.0150 | _ | 0.0200 | _ | 0.0230 | _ | 0.0260 | _ |
| | 10 | 0.0069 | 53.1 | 0.0100 | 48.8 | 0.0119 | 44.3 | 0.0149 | 41.4 |
| | 20 | 0.0060 | 56.7 | 0.0090 | 53.6 | 0.0110 | 50.0 | 0.0140 | 46.0 |
| | 40 | 0.0022 | 85.2 | 0.0033 | 82.4 | 0.0048 | 71.7 | 0.0083 | 67.9 |
| | 60 | 0.0020 | 87.6 | 0.0030 | 83.5 | 0.0040 | 75.8 | 0.0070 | 72.6 |
| | 80 | 0.0014 | 90.7 | 0.0029 | 84.4 | 0.0039 | 82.8 | 0.0054 | 78.6 |
| | 100 | 0.0010 | 93.3 | 0.0020 | 87.6 | 0.0030 | 84.2 | 0.0050 | 80.1 |

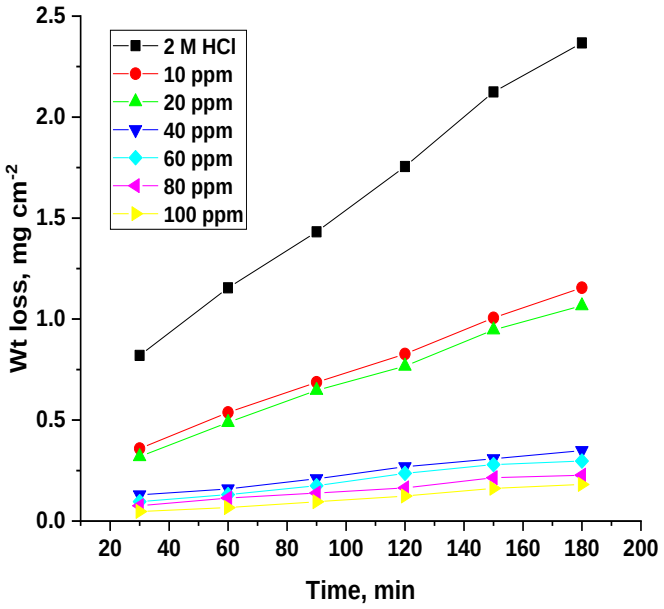


**Figure 1.** WL – time curves in the absence and presence various concentrations of *C. bonariensis* extract at 30˚C.

*3.1.2. Adsorption Isotherms*

Several isotherm models were evaluated to examine the interaction between *C. bonariensis* extract and the CS surface. The Langmuir isotherm was the appropriate model to illustrate the adsorption process. The expression of Langmuir model is [34]:

$$C/\theta = 1/K_{ads} + C \quad (6)$$

where "θ is the surface coverage, a is the parameter of molecular interaction, $K_{ads}$ is equilibrium constant of adsorption and C is concentration of inhibitor." By plotting θ with log C Fig. 2, straight lines were acquired with intercept 2.303/a log $K_{ads}$ and slope of lines 2.303/a.

The $K_{ads}$ is associated with Gibbs free energy ($-\Delta G^{\circ}_{ads}$) by this equation [35-36]:

$$log\, K_{ads} = -log\, 55.5 - \frac{\Delta G^{\circ}_{ads}}{2.303RT} \quad (7)$$

where "R is the constant of universal gas, T is the absolute temperature, and the value of 55.5 is equal to water concentration."

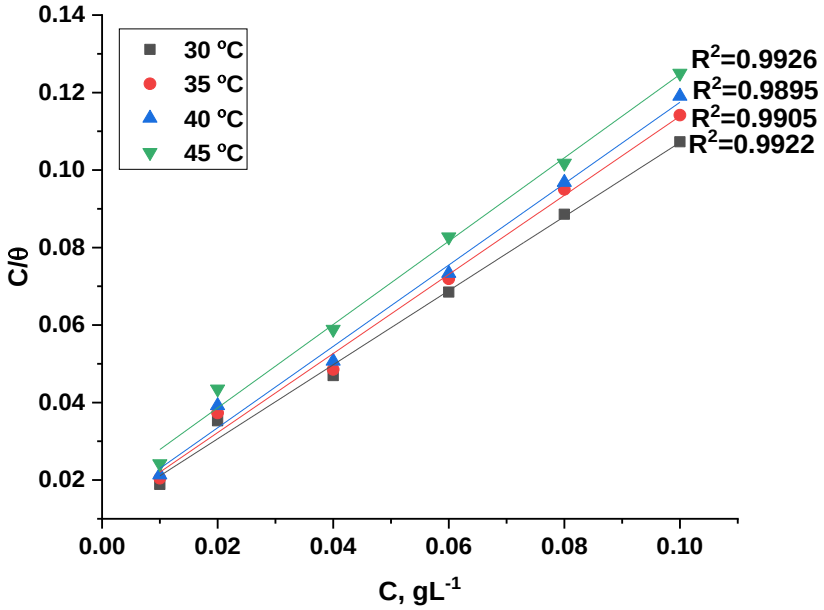


**Figure 2.** Langmuir's adsorption isotherm of *C. bonariensis* on the CS of at different temperatures.

**Table 2.** Data of thermodynamic adsorption parameters of *C. bonariensis* extract on CS surface in 2 M HCl at different temperatures.

| **Inhibitor** | **Temp.** K | **$K_{ads.} \times 10^4$** $mol^{-1}$ | **$-\Delta G^{\circ}_{ads}$** kJ $mol^{-1}$ |
|---|---|---|---|
| *C. bonariensis* | 303 | 86.80 | 21.36 |
| | 308 | 84.46 | 21.64 |
| | 313 | 80.00 | 21.85 |
| | 318 | 58.37 | 21.37 |

From the data of thermodynamic adsorption parameters found in Table 2, the following notes can be concluded:

The negative sign of $\Delta G^{\circ}_{ads}$ showed that the absorption of *C. bonariensis* extract on the surface of metal [37] was spontaneous. The results of $\Delta G^{\circ}_{ads}$ are negative approximately -21 kJ $mol^{-1}$ which affiliated with the physical absorption reaction resulting from Van der Waals attraction force [38-39].

*3.1.3 Activation Parameters*

The thermodynamic parameters of the excitation state of the destructive reaction were evaluated from WL measurements at varied temperatures. The activation energies ($E_a^*$) of corrosion process were given from Arrhenius expression as follows [40]:

$$\log k_{corr} = \left(\frac{-E_a^*}{2.303RT}\right) + \log A \qquad (8)$$

Where "$E_a^*$ is the energy of activation, A is the factor of Arrhenius pre-exponential and $k_{corr}$ is the CR" obtained from WL measurements. Fig.3. showed (log $k_{corr}$) versus (1/T) for *C. bonariensis* extract and straight lines were acquired. The obtained data of $E_a^*$ was recorded in Table 3 , with raising the concentration of *C. bonariensis* extract, the $E^*_a$ values increases which indicate the formation energy barrier due to adsorption of the inhibitor molecules [41,42].

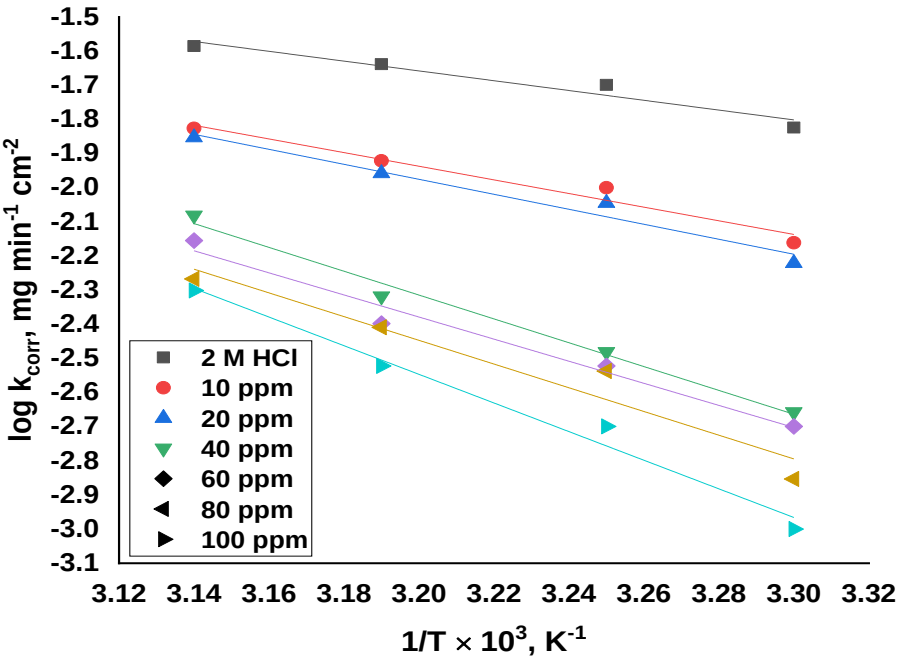


**Figure 3.** 1/T versus $k_{corr}$ for absence and presence of various concentrations of *C. bonariensis* extract.

The activation entropy $\Delta S^*$ and activation enthalpy $\Delta H^*$ were estimated by transition state equation [43]:

$$\log k_{corr} = \log\left(\frac{R}{Nh}\right) + \frac{\Delta S^*}{2.303R} + \frac{\Delta H^*}{2.303RT} \quad (9)$$

Where "N is Avogadro's number, h is Planck's constant, $\Delta H^*$ is enthalpy of activation and $\Delta S^*$ is the activation entropy". Fig.4 displayed (log $k_{corr}$ /T) against (1/T) for *C. bonariensis* extract. We can determine the activation parameters from values of slope and intercept of straight lines. The obtained values of activation parameters were recorded in Table 3. The positive sign of $\Delta H^*$ indicates the endothermic reaction of the degradation procedure of CS [44]. The negative values of $\Delta S^*$ indicated that the inhibitor molecule are presented in associated form (i.e., active complex [inhibitor-metal]) rather than dissociated form in solution [45,46].

**Table 3.** Parameters for activation of CS in the absence and presence different concentrations of *C. bonariensis* extract in 2 M HCl.

| **Inhibitor** | **Conc.,** ppm | $\mathbf{E_a^*}$ kJ mol$^{-1}$ | $\mathbf{\Delta H^*}$ kJ mol$^{-1}$ | $\mathbf{-\Delta S^*}$ J mol$^{-1}$ K$^{-1}$ |
|---|---|---|---|---|
| *C. bonariensis* | 2 M HCl | 27.47 | 5.38 | 190.22 |
| | 10 | 38.23 | 8.15 | 182.98 |
| | 20 | 42.02 | 9.32 | 179.48 |
| | 40 | 66.84 | 16.44 | 158.71 |
| | 60 | 61.94 | 14.72 | 164.64 |
| | 80 | 66.49 | 15.87 | 161.36 |
| | 100 | 80.28 | 20.14 | 148.30 |

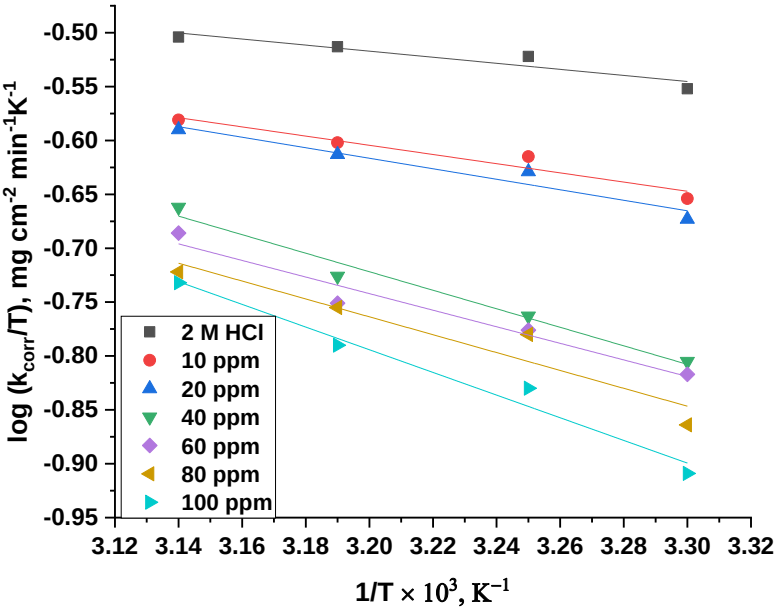


**Figure 4.** (1/T) against log ($k_{corr}$/T) curves in absence and presence of various concentrations of *C. bonariensis* extract.

### *3.2. Electrochemical Measurements*

#### *3.2.1. Potentiodynamic Polarization Measurements*

Tafel polarization curves of CS in 2 M HCl media before and after treating with various concentrations of *C. bonariensis* extract at 25°C was shown in Fig.5. The figure showed that the current densities of anodic and cathodic branches decrease by adding different concentrations of *C. bonariensis* extract indicating the anodic and cathodic reactions were inhibited by plant extract. The electrochemical parameters $E_{corr}$, $\beta_a$ & $\beta_c$, θ, IE % and $i_{corr}$ were estimated and established in Table 4. The acquired data showed that the current of corrosion ($i_{corr}$) was decreased by addition of present extract leading to

decrease in the CR and increase of IE% owing to the establishment of protective adsorbed layer of the plant extract. While the values of $E_{corr}$ were not significantly changed, so the *C. bonariensis* extract performed as mixed type of inhibitor indicating that the *C. bonariensis* extract hindered both $H_2$ evolution process (cathodic reaction) and CS dissolution process (anodic reaction) [45]. Moreover, the non-significant change of $\beta_a$ and $\beta_c$ revealing that the *C. bonariensis* extract does not modify the mechanism of CS corrosion in 2 M HCl [46].

**Table 4.** Electrochemical parameter, $i_{corr}$, $E_{corr}$, $\beta_a$, $\beta_c$, $k_{corr}$, θ and IE % of CS in 2 M HCl for presence and absence of various concentrations of *C. bonariensis* extract.

| Inhibitor | conc., ppm | − $E_{corr}$, mV vs. SCE | $\beta_a$ mV $dec^{-1}$ | $\beta_c$ mV $dec^{-1}$ | $i_{corr}$, μA $m^{-2}$ | θ | %$IE_{PDP}$ |
|---|---|---|---|---|---|---|---|
| *C. bonariensis* | 2 M HCl | 431 | 76 | 115 | 150 | - | - |
| | 10 | 441 | 106 | 120 | 56.9 | 0.621 | 62.1 |
| | 20 | 442 | 109 | 123 | 48.4 | 0.677 | 67.7 |
| | 40 | 445 | 108 | 127 | 38.4 | 0.744 | 74.4 |
| | 60 | 442 | 123 | 121 | 30.1 | 0.799 | 79.9 |
| | 80 | 445 | 134 | 129 | 15.9 | 0.894 | 89.4 |
| | 100 | 446 | 139 | 132 | 10.2 | 0.932 | 93.2 |

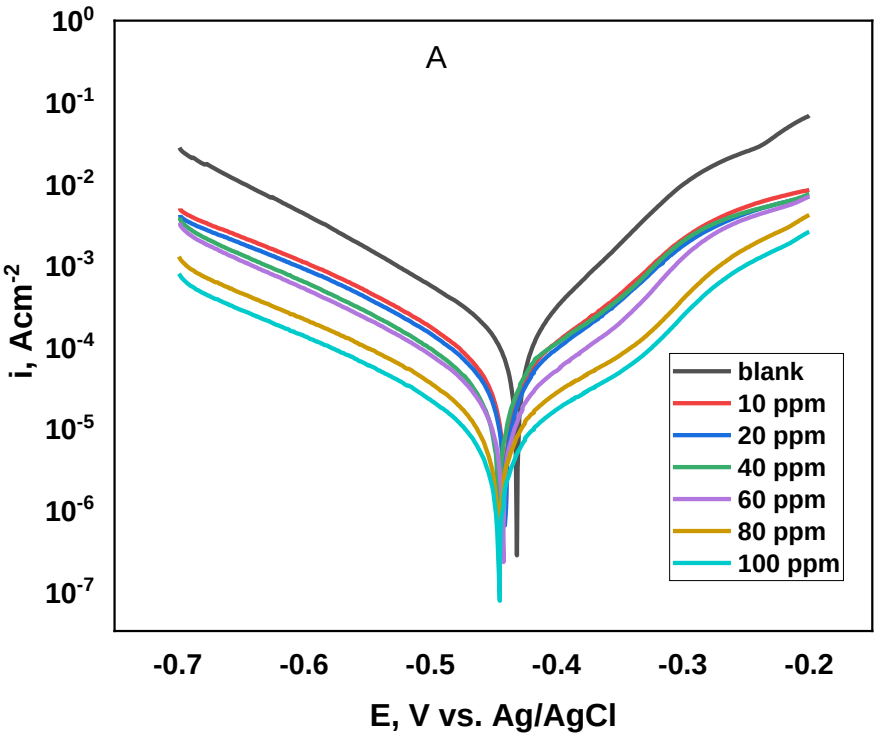


**Figure 5.** PP plots for CS in the absence and presence of various concentrations of *C. bonariensis* at 25˚C.

*3.2.2. Electrochemical Impedance (EIS) Measurements*

The Nyquist and Bode plots of CS before and after adding various dosages of *C. bonariensis* extract are cleared in Fig. 6-a and 6-b individually. Nyquist plot showed one discouraged capacitive circle and Bode plot showed one stage point greatest which is credited to the presence of one time steady in the corrosion interaction identified with the electrical twofold layer presence in metal– solution interface [47].

The Fig. 6-a curves showed that there is gradual rise in the shape of each semicircle of the Nyquist curves by raising the concentration of the present extract. The curves which resulted from Nyquist plots are not completely semicircle these because of roughness and homogeneity of the electrode surface [47].

In Fig. 7, the equivalent circuit examined the EIS spectra for CS corrosion in 2 M HCl before and after adding *C. bonariensis* extract included $R_s$ (solution resistance), $R_{ct}$ (charge transfer resistance), and CPE (constant phase element for a double layer). The following describes the impedance as a function of CPE [48]:

$$C_{dl} = Y_0 (\omega_{max})^{n-1} \quad (10)$$

Where, "$\omega_{max}$ denotes the angular frequency when the imaginary component of the impedance at its maximum value, $Y_0$ is the magnitude of CPE, and n is a CPE exponent" relies on the character of the metal surface.

The %IE was estimated by using this Eq. [49]:

$$\%IE_{EIS} = \frac{R_{ct\,(inh)} - R_{ct}}{R_{ct\,(inh)}} \times 100 \quad (11)$$

Where "$R_{ct}$ is the resistance of charge transfer and $C_{dl}$ is the capacitance of double layer." The data of (IE %, θ, $R_{ct}$ and $C_{dl}$) are listed in Table 5. These data may prove there is an increasing in ($R_{ct}$) by increasing *C. bonariensis* extract concentration demonstrates a rise in their protecting versus the corrosion by reason of the construction of adsorbed protective layer [50]. While the ($C_{dl}$) decreased owing to the exchange the water molecules by inhibitor molecules leading to an increase in the electrical double layer thickness and decrease in dielectric constant as the concentrations of *C. bonariensis* extract increased [51].

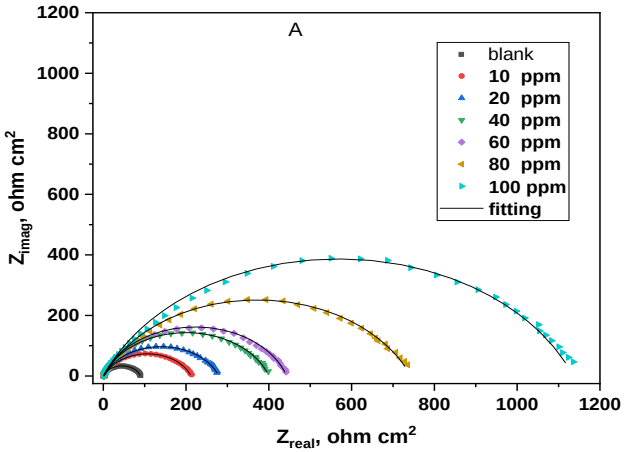


**Figure 6-a.** Nyquist curves for CS in the absence and presence of various concentrations of *C. bonariensis* extract.

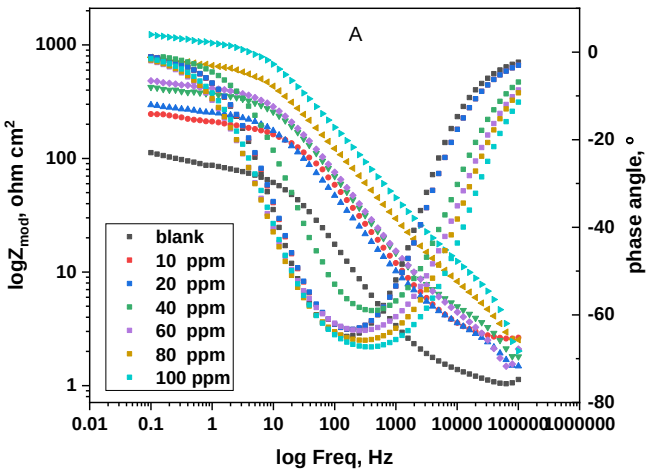


**Figure 6-b.** Bode curves for CS in 2 M HCl for absence and presence of various concentrations of *C. bonariensis* extract.

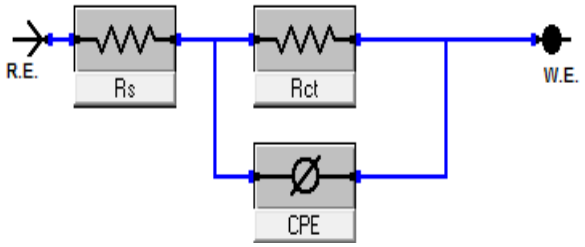


**Figure 7.** Equivalent circuit model

**Table 5.** Data obtained from EIS measurements for CS corrosion in the absence and presence of various concentrations of *C. bonariensis* extract at 25˚C.

| Inhibitor | Conc. ppm | $R_{ct}$, Ω cm$^2$ | $C_{dl}$, µF cm$^2$ | Θ | %$IE_{EIS}$ |
|---|---|---|---|---|---|
| *C. bonariensis* | 2 M HCl | 89.8 | 335.2 | - | - |
| | 10 | 209.7 | 144.0 | 0.572 | 57.2 |
| | 20 | 278.3 | 133.5 | 0.677 | 67.7 |
| | 40 | 402.8 | 123.1 | 0.777 | 77.7 |
| | 60 | 450.4 | 93.8 | 0.801 | 80.1 |
| | 80 | 747.2 | 87.9 | 0.880 | 88.0 |
| | 100 | 1198.0 | 52.5 | 0.925 | 92.5 |

### *3.3. The surface Examination*

#### *3.3.1. Atomic Force Microscopy (AFM)*

The surface morphology of CS was examined by AFM technique when immersed in a media of 2 M HCl with and without 100 ppm of *C. bonariensis* extract and for pure CS sample after treatment by physical methods as WL measurements. Fig 8-a showed the 3-D image for pure CS surface. Fig 8-b

showed the 3-D image for CS surface in 2 M HCl for 24 hours. In this image, we can see that the surface was more corroded and destroyed compared to smooth surface of pure CS. In case of added 100 ppm of investigated extract, Fig 8-c showed the 3-D image for the CS surface was less destroyed and becomes smoother than in case of CS in corrosive media. The average roughness of the polished CS, CS surface in 2 M HCl before and after adding the present inhibitor was measured to be 17.47 nm, 1134.91 nm and 135.32 nm, alternatively. The three-dimensional images and other results demonstrate the adsorption of the *C. bonariensis* extract on the surface of the CS.

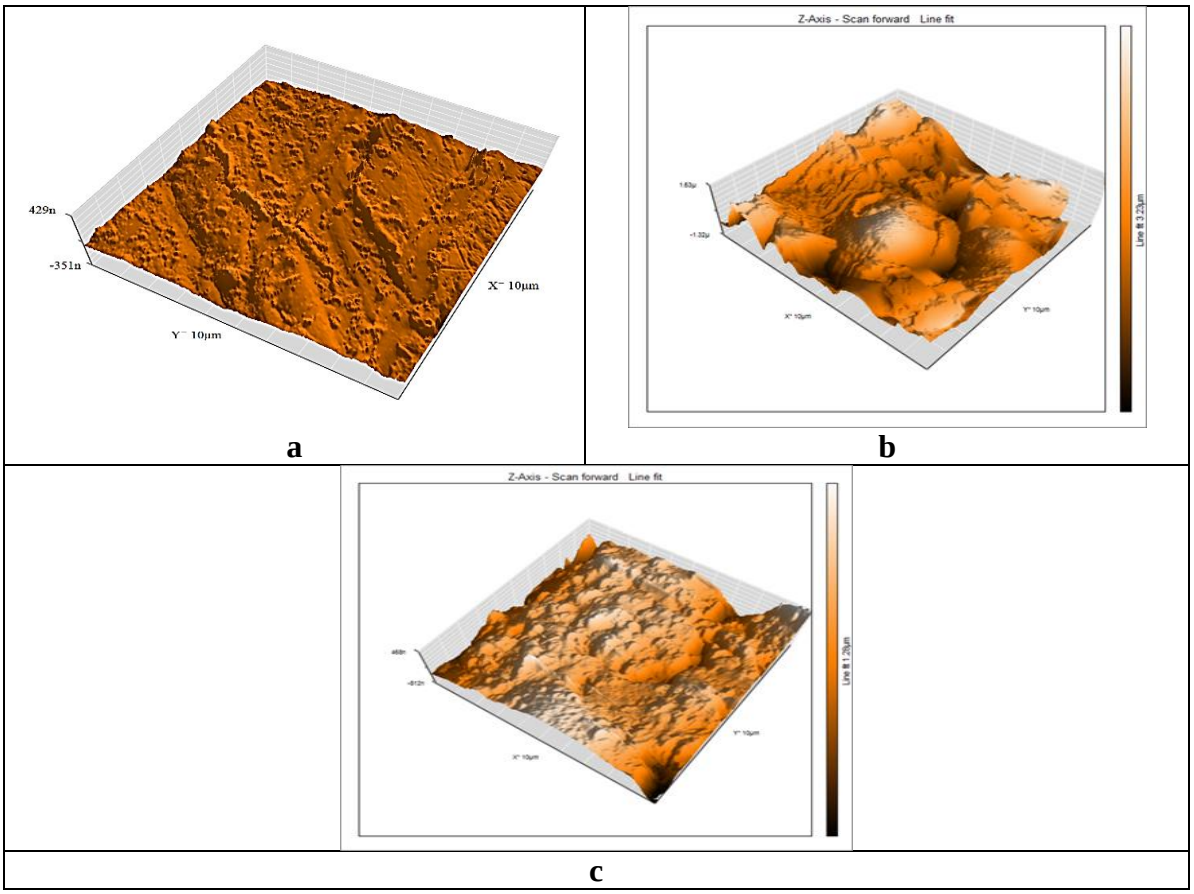


**Figure 8.** AFM images for CS (a) for pure surface, (b) after one day immersion in 2 M HCl solution and (c) presence of 100 ppm *C. bonariensis* extract.

*3.3.2. Scanning Electron Microscopy Studies (SEM)*

The photo of the carbon steel surface cleaned before immersion in the 2M HCl array is shown in in Fig. 9. The photo shows that the surface is smooth and free of pitting Fig. 9a. The surface photo of the carbon steel immersed in 2M HCl array is shown in Fig. 9b. The photo reveals that the surface is firmly damaged and there is no *C. bonariensis*. The photo of the carbon steel surface after immersing in the 2M HCl array containing 100 ppm *C. bonariensis* is shown in Fig. 9c. It was found that the faceting observed in figures disappeared and the surface was free from pits, and it was smooth. It can be concluded from Fig11c that the corrosion is greatly reduced in the presence of *C. bonariensis*, thus when

*C. bonariensis* is present in the medium, the corrosion is strongly inhibited. Figs. 10a–c EDX spectrum, in the absence and presence of *C. bonariensis*. In the presence of *C. bonariensis* in Figures 10b and 10c, the EDX spectrum shows the additional line characteristics of O and Cl. In addition, the intensity of the C, signal has been improved. The appearance of the Cl and O signals and this improvement in the C signal are due to the atoms of Cl, C and O that form *C. bonariensis*. This indicates that the inhibitory molecules have been adsorbed onto the metal surface. The data obtained from the spectra are listed in Table 6. The spectrum also shows that the Fe peak is significantly suppressed in the presence of the inhibitor due to the superimposed inhibitor film. These results support the results of electrochemical measurements, indicating that the surface film inhibits the dissolution of metals, thereby delaying the hydrogen evolution reaction. The EDX spectrum shows characteristic peaks (Fe, O, and Cl) attributed to general corrosion in dilute hydrochloric acid.

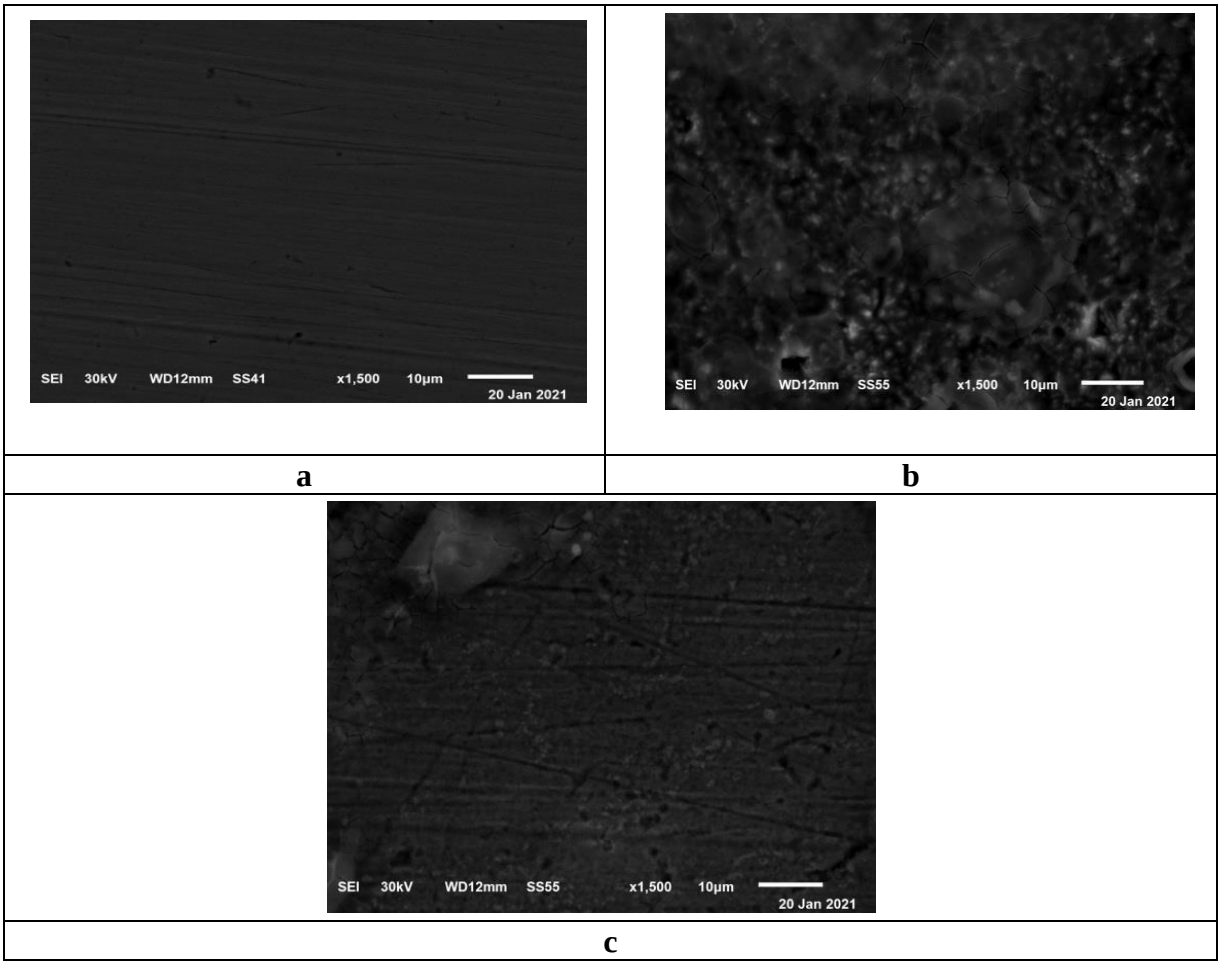


**Figure 9.** SEM micrograph of the carbon steel surface (a) before immersion in 2M HCl, (b) after immersion in 2M HCl for 24 hours and (c) after immersion in 2M HCl + 100 ppm for 24 hours of *C. bonariensis* at 25 ° C.

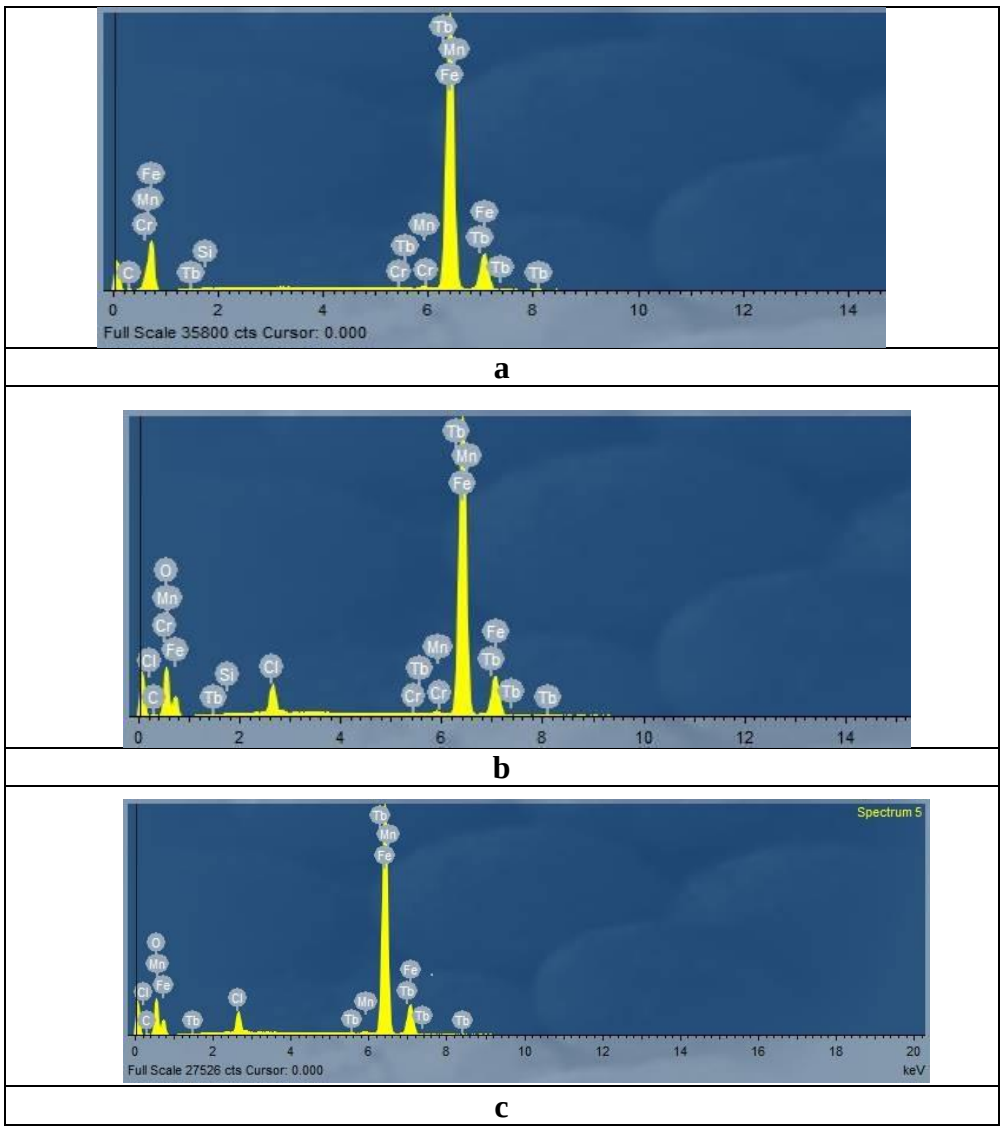


**Figure 10.** EDX spectrum of CS surface: (a) before immersion in 2 M HCl, (b) after immersion in 2 M HCl for 24 hours and (c) after immersion in 2 M HCl + 100 ppm *C. bonariensis* at 25°C.

**Table 6.** Surface composition (wt %) of CS before and after immersion in 2 M HCl without and with 100 ppm of *C. bonariensis* at 25 °C.

| (Mass %) | Fe | C | O | Mn | Cl | Tb | Si | Cr |
|---|---|---|---|---|---|---|---|---|
| **Pure** | 78.78 | 16.41 | - | 0.39 | - | 3.75 | 0.52 | 0.15 |
| **blank** | 35.28 | 8.63 | 50.54 | 0.20 | 3.37 | 1.64 | 0.26 | 0.08 |
| ***C. bonariensis*** | 34.87 | 10.39 | 49.73 | 0.15 | 3.23 | 1.63 | - | - |

*3.4. Corrosion inhibition mechanism*

The leaves of *C. bonariensis* plant mainly have alkaloids, terpenoids, phenolic acid derivatives, iridoid glycosides, flavonoids, and fatty acids. These constituents contain hetero atoms like O and N

which having lone pairs of electrons as well as benzene rings which having π-electrons. Causes a strong affinity to reduce the dissolution of metal and inhibit the evolution of hydrogen. It is well known that the surface of steel is positively charged in acid solution [47,50]. Therefore, the protonated components of the extract of *C. bonariensis* in 2 M HCl are difficult to approach the steel surface. It is positively charged due to electrostatic repulsion. The presence of chloride ions will generate an excess of negative charges towards the solution and enhance the further adsorption of the protonation inhibitor through electrostatic interaction with the negatively charged metal surface. This interaction mode is consistent with the value of $\Delta G°_{ads}$, where the adsorption of the *C. bonariensis* component is physical adsorption.

## 4. CONCLUSIONS

From the obtained results, we can conclude that:

*Conyza bonariensis* extract is considered as an effective green corrosion inhibitor (93.3% with 100 ppm) for the CS in 2 M HCl.

The WL method explained that if the concentration of *C. bonariensis* increased and the temperature decreased, the inhibition efficiency would also increase.

The adsorption of *C. bonariensis* on the CS surface is physisorption according to the values of $\Delta G^{\circ}_{ads}$.

PP curves showed the ability of *C. bonariensis* plant to serve as a mixed-type inhibitor.

EIS results confirmed the adsorption of *C. bonariensis* on CS surface by lowering the values of $C_{dl}$ with increasing of the concentration.

Surface morphology analyses approved the adsorption of *C. bonariensis* on the CS surface in 2 M HCl.

## References

1. N. E. Basiony, A.Elgendy, H. Nady, M.A.Migahed, E.G. Zaki, *RSC advances*, 9 (2019) 10473.
2. J. M. Praveena, R. J. Rathish, S. Rajendran, S. S Kumaran, G.Singh, A. Al-Hashem, *In Corrosion Protection at the Nanoscale*, (2020) 107.
3. A. Singh, K. R Ansari, D. S. Chauhan, M. A Quraishi, H. Lgaz, I. M. Chung, *Journal of colloid and interface science*, *560*(2020) 225.
4. R. Haldhar, D. Prasad, I. Bahadur, O. Dagdag, A. Berisha, *Journal of Molecular Liquids*, 323 (2021) 114958.
5. N. S.Palsson, K. Wongpinkaew, P. Khamsuk, S. Sorachot, W. Pongsaksawad, *Materials and Corrosion*, 71 (2020)1019.
6. J.Wang, D.Liu, S.Cao, S.Pan, H.Luo, T.Wang, J.Gui, *Journal of Molecular Liquids*, 312 (2020)113436.
7. J. Qiu, D. D Macdonald, Y. Xu, L.Sun, *Materials and Corrosion*, 72 (2021) 107.
8. M. Abdallah, H. M. Altass, B. A. Al Jahdaly, M. M.Salem, *Green Chemistry Letters and Reviews*, 11 (2018)189.
9. A. Dehghani, G. Bahlakeh, B. Ramezanzadeh, M. Ramezanzadeh, *Journal of the Taiwan Institute of Chemical Engineers*, 100 (2019) 239.

10. X Zuo, W.Li, W.Luo, X.Zhang, Y.Qiang, J.Zhang, B.Tan, *Journal of Molecular Liquids*, 321 (2021)114914.
11. P. E. Alvarez, M.V. Fiori-Bimbi, A.Neske, S.A.Brandán, C. A Gervasi, *Journal of industrial and engineering chemistry*, *58*(2018) 92.
12. Q.Wang, B.Tan, H.Bao, Y.Xie,Y.Mou, , P.Li, W.Yang, *Bioelectrochemistry*, *128* (2019) 49
13. A. S. Fouda, M. M. Hegazi, A.El-Azaly, *Int. J. Electrochem. Sci.*, *14* (2019) 4668.
14. G.Bahlakeh, B.Ramezanzadeh, A.Dehghani, M.Ramezanzadeh, *Journal of Molecular Liquids*, *283*(2019) 174.
15. M. A. Deyab, E. Guibal, *Scientific reports*, *10* (2020) 1.
16. L. K.Ojha, B .Tüzün, J. Bhawsar, *Journal of bio-and tribo-corrosion*, *6* (2020) 1.
17. A. Miralrio, A. Espinoza Vázquez, *Processes*, *8* (2020) 942.
18. A.M.Abdel-Gaber, H.T.Rahal,F.T.Beqai, *International Journal of Industrial Chemistry*, (2020) 1
19. M. A. da Costa, J. S. D.Gois, , I. M .Toaldo, A. C. F.Bauerfeldt, D. B .Batista, M. T.Bordignon-Luiz, L. F. D. Senna, *Materials Research*, *23* (2020).
20. A.Berrissoul, A. Ouarhach, F. Benhiba, A. Romane, A. Zarrouk, A.Guenbour, A. Dafali, *Journal of Molecular Liquids*, *313* (2020) 113493.
21. R. V.Espinoza, J. Peñarreta, M.Quijano-Avilés, A. B. Lucas, I.Chóez-Guaranda, P. M.Santana, *Revista Facultad Nacional de Agronomía Medellín*, *73* (2020) 9305.
22. D.Loura, S. Florentine, B. S. Chauhan, *Weed Science*, *68* (2020) 411.
23. F. Valencia Gredilla, M.L.Supiciche, G.R.Chantre, J.Recasens, A.Royo Esnal, *Annals of Applied Biology*, *176* (2020) 36.
24. S. L.Schechtel, V. C. R de Matos, J. S. Santos, T. M. Cruz, M. B. Marques, M.Wen, D. Granato, *Journal of food science*, *84* (2019) 3473.
25. T. F. O.da Silva, S. M. S. Lopes, J. C.Castro, G. Krausová, J.Smolova, J. W. P. Carneiro, A.J.B.deOliveira, *Bioactive Carbohydrates and Dietary Fibre*, 25 (2021)100257.
26. C. M.Fernandes, M.V.P.deMello, N. E.dos Santos, A. M. T.de Souza, M. Lanznaster, E. A.Ponzio, *Materials and Corrosion*, *71* (2020) 280.
27. A.Dehghani, G.Bahlakeh, B.Ramezanzadeh, M. Ramezanzadeh, *Journal of Molecular Liquids*, *310*(2020) 113221.
28. V.Saraswat, M. Yadav, *Journal of Molecular Liquids*, 297(2020) 111883.
29. M.Ouakki, M.Galai, M. Rbaa, A. S. Abousalem, B. Lakhrissi, M. E. Touhami, M. Cherkaoui, Journal *of Molecular Liquids*, 319(2020) 114063.
30. S. Al-Nami, A. E. A. S. Fouda, *Int. J. Electrochem. Sci*, 15(2020) 1187.
31. O. A.Elgyar, A. M.Ouf, A.El-Hossiany, A. E. A. S. Fouda, *Biointerface Research in Applied Chemistry* , 11(2021)14333.
32. M.T. Saeed, M.Saleem, S.Usmani, I. A.Malik, F. A. Al-Shammari, K. M. Deen, Journal *of King Saud University-Science*, 31 (2019) 1344.
33. M.P.Asfia, M.Rezaei, G.Bahlakeh, *Journal of Molecular Liquids*, 315 (2020) 113679.
34. E. S. F. A.El-Aziz, R. S.Mahmoud, H.Ibrahim, A. R. Ezzat, *Zaštita materijala*, 61 (2020)192.
35. J.Aslam, R.Aslam, I. H.Lone, N. R.Radwan, M.Mobin, A.Aslam, A. A.Alzulaibani, *Journal of Materials Research and Technology*, 9 (2020) 4061.
36. J.Poon, D.C.Madden, R.J.Welbourn, F.J.Allen, F.Khan, H.Sonke, S M. Clarke, *Surface and Coatings Technology*, *410* (2021)126970.
37. S.Bashir, A.Thakur, H. Lgaz, I. M. Chung, A.Kumar, *Surfaces and Interfaces*, 20 (2020) 100542.
38. M.Rbaa, F. Benhiba, M.Galai, A.S. Abousalem,M.Ouakki,C.H.Lai,A.Zarrouk,*ChemicalPhysics Letters*, *754* (2020)137771.
39. S.Bashir, A. Thakur, H.Lgaz, I. M.Chung, A.Kumar, *Arabian Journal for Science and Engineering*, *45* (2020) 4773.
40. A.Salhi, S.Tighadouini, M.El-Massaoudi, M. Elbelghiti, A.Bouyanzer, S. Radi, A. Zarrouk, *Journal of Molecular Liquids*, *248* (2017) 340.

41. M. H.Sliem, M.Afifi, A. B.Radwan, E. M.Fayyad, M. F.Shibl, F. E. T. Heakal, A. M. Abdullah, *Scientific reports*, *9* (2019) 1.
42. A. Louroubi, A. Nayad, A. Hasnaoui, R. Idouhli, A. Abouelfida, L. El Firdoussi,M. Ait Ali, *Journal of Chemistry*, 2021 (2021)1
43. C.V.Maridevarmath, H.Malimath, *the Journal of Chemical Thermodynamics*, 144 (2020) 106068.
44. H.Zhu, Y.Huo, W.Wang, X.He, S.Fang, Y.Zhang, *Process Safety and Environmental Protection*, 148 (2021) 624.
45. C. B. N. Unnisa, S. Chitra, G. N.Devi, A. Kiruthika, S. M.Roopan, V.Hemapriya, M. Prabakaran, *Research on Chemical Intermediates*, 45 (2019) 5425.
46. K. Shalabi, A. M.Helmy, A. H.El-Askalany, M.M.Shahb, *Journal of Molecular Liquids*, 293 (2019) 111480.
47. A. M.Eid, S.Shaaban, K.Shalabi, Journal *of Molecular Liquids*, 298 (2020)111980.
48. Y.Qiang, S. Zhang, B.Tan, S. Chen. , *Corrosion Science*, *133* (2018) 6.
49. K. Shalabi, A. A.Nazeer, *Journal of Molecular Structure*, 1195(2019) 863.
50. Y. M. Abdallah, K. Shalabi, N. M. Bayoumy, *Journal of Molecular Structure*, 1171 (2018) 658.
51. Z.Sanaei, G.Bahlakeh, B. Ramezanzadeh, M. Ramezanzadeh, *Journal of Molecular Liquids*, 290 (2019) 111176.